

Effect of BAPTA and EGTA on Inactivation of I_{Ca} in a Model of Rat Ventricular Myocyte

Pásek M^{1,2}, Šimurda J^{1,3}, Orchard C H⁴

¹ Department of Physiology, Faculty of Medicine, Masaryk University, Brno, Czech Republic

² Institute of Thermomechanics - branch Brno, Czech Academy of Science, Brno, Czech Republic

³ Department of Biomedical Engineering, University of Technology, Brno, Czech Republic

⁴ Department of Physiology and Pharmacology, University of Bristol, Bristol, United Kingdom.

mpasek@med.muni.cz

Abstract. An existing model of the rat ventricular myocyte was modified to reproduce the experimentally observed differential effects of the fast and slow exogenous Ca^{2+} buffers BAPTA and EGTA on inactivation of I_{Ca} and to investigate the possible cause. The results of the simulations suggest that the different potencies of EGTA and BAPTA on inactivation of I_{Ca} are due to their different rates of Ca^{2+} binding, and thus different intracellular gradients of bound and unbound buffer, causing different rates of diffusion of bound and unbound buffer out of and into the dyadic space. The consequent difference in suppression of the Ca^{2+} transient in the dyadic space caused different rates of Ca^{2+} -induced inactivation of I_{Ca} in the presence of the two buffers.

1 Introduction

In cardiac ventricular myocytes, the fast Ca^{2+} buffer BAPTA has a greater effect than the slow Ca^{2+} buffer EGTA on inactivation of the L-type Ca^{2+} current, I_{Ca} (e.g. [1, 2]). The aim of the present study was to refine an existing model of the rat ventricular myocyte [3] to reproduce the published differential effects of BAPTA and EGTA on inactivation of I_{Ca} in the rat ventricular myocyte (Fig 1, [1]) and to investigate the possible cause.

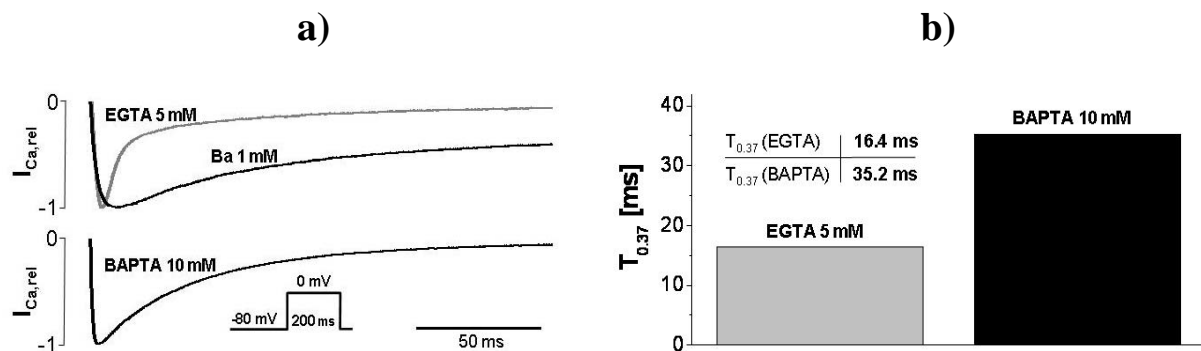


Fig 1. Inactivation of I_{Ca} in the presence of intracellular EGTA (5 mM) or BAPTA (10 mM) in rat ventricular myocytes (data adopted from [1]). (a) I_{Ca} recorded during 200 ms depolarising pulse from -80 mV to 0 mV at room temperature. (b) The kinetics of I_{Ca} -inactivation were characterized by the time required for the current to decay to 0.37 of the peak amplitude ($T_{0.37}$). I_{Ca} -inactivation was substantially slowed in the presence of 10 mM BAPTA, causing significant prolongation of $T_{0.37}$ (35.2 ms versus 16.4 ms in the presence of 5 mM EGTA). 1 mM Ba was used to illustrate the time course of I_{Ca} in the absence of Ca^{2+} -dependent inactivation.

2 Methods

The description of intracellular Ca^{2+} dynamics in the original model of the rat ventricular myocyte [3] was modified to comply with recent experimental data. The principal modifications to the model (see Fig 2) were: (i) reformulation of the description of sarcoplasmic reticulum (SR) Ca^{2+} -release according to [4]; (ii) reformulation of the description of voltage and Ca^{2+} dependent inactivation of I_{Ca} to simulate the experimental data of [1]; (iii) modification of the parameters of the SR Ca-pump to give the relation between free Ca^{2+} in the cytosol and SR described by [5]; (iv) incorporation of equations controlling exchange of free EGTA and Ca^{2+} -EGTA and of free BAPTA and Ca^{2+} -BAPTA between the pipette, cytosol and dyadic space.

To mimic the experimental conditions specified in [1], the following ion concentrations in extracellular bulk compartment and in the pipette were set in the model: $[\text{Ca}^{2+}]_e = 1 \text{ mM}$, $[\text{Na}^+]_e \approx 0 \text{ mM}$, $[\text{K}^+]_e \approx 0 \text{ mM}$, $[\text{Ca}^{2+}]_p = 0.5 \text{ nM}$. The intracellular concentrations $[\text{Na}^+]_i$ and $[\text{K}^+]_i$ were fixed at levels close to zero to reflect their dialysis by the pipette. K^+ currents were disabled because they were blocked experimentally using Cs in the pipette solution.

To compare the simulated results with experimental data [1] the kinetics of I_{Ca} -inactivation were characterized by the time required for the current to decay to 0.37 of the peak amplitude ($T_{0.37}$).

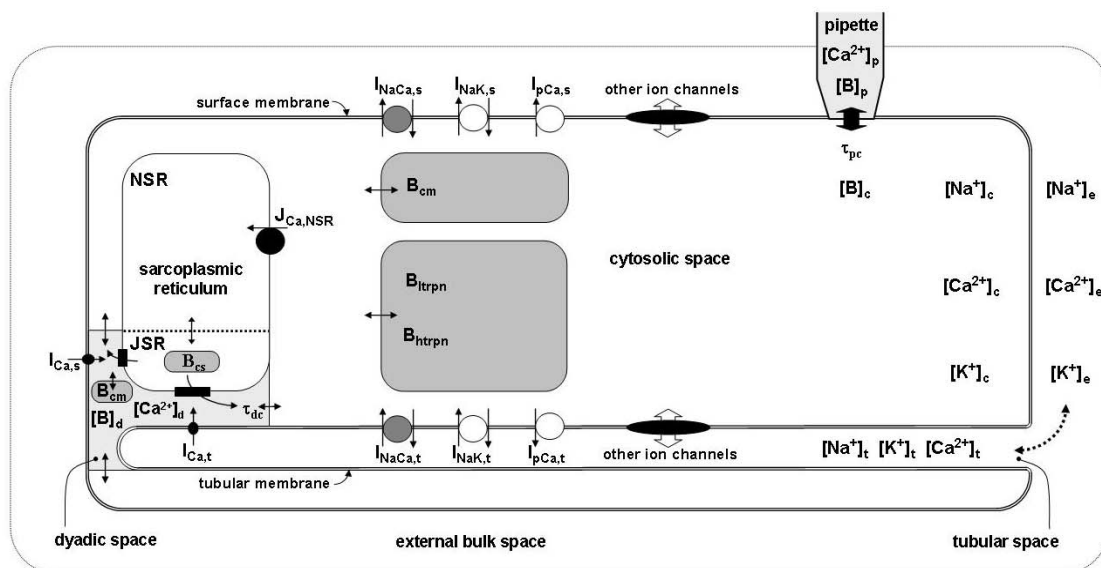


Fig 2. Schematic diagram of the rat ventricular cell model. The description of electrical activity of surface (s) and t-tubular (t) membrane comprises formulations of the following ionic currents: I_{Ca} , calcium inward current; I_{Kto} , time-dependent transient outward potassium current; I_{Kss} , steady-state outward potassium current; I_{Kf} , hyperpolarization-activated current; I_{K1} , time-independent inward rectifier potassium current; I_{Nab} , background sodium current; I_{Cab} , background calcium current; I_{Kb} , background potassium current; I_{NaCa} , Na^+ - Ca^{2+} -exchanger current; I_{NaK} , electrogenic Na^+ - K^+ -ATPase pump current; I_{pCa} , sarcolemmal Ca-pump current. The intracellular space contains the cytosol, the subspace, the Ca^{2+} -uptake and Ca^{2+} -release compartments of sarcoplasmic reticulum (NSR, JSR) and endogenous Ca^{2+} buffers calmodulin (B_{cm}), troponin (B_{itrpn} , B_{htrpn}) and calsequestrin (B_{cs}). The presence of exogenous Ca^{2+} buffers (EGTA or BAPTA) in the pipette, cytosol and subspace is marked by symbols $[B]_p$, $[B]_c$ and $[B]_d$, respectively. The small filled rectangles in JSR membrane represent ryanodine receptors. The small bi-directional arrows denote Ca^{2+} diffusion. The dashed arrow represents ionic diffusion between the tubular and the bulk space.

3 Results

The model reconstruction of experimental results showing the normalized responses of I_{Ca} to a depolarizing pulse from -80 to 0 mV under control conditions and in the presence of EGTA (5 mM) or BAPTA (10 mM) is illustrated in Fig. 3a. The values of $T_{0.37}$ determined from simulated traces of I_{Ca} in the presence of the buffers are shown in Fig. 3b.

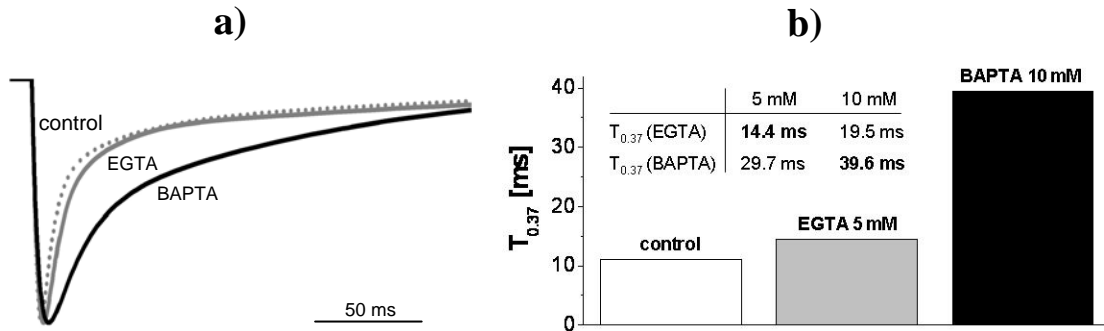


Fig 3. Effect of EGTA and BAPTA on I_{Ca} -inactivation in the model. (a) Superimposed normalized responses of I_{Ca} to a depolarizing pulse from -80 to 0 mV in control conditions and under the effect of 5 mM EGTA and 10 mM BAPTA. (b) Values of $T_{0.37}$ characterizing the rate of I_{Ca} -inactivation.

4 Discussion

In the model, both buffers inhibited the cytosolic Ca^{2+} -transient, and thus contraction. However, only BAPTA inhibited effectively the rise of Ca^{2+} in the dyadic space, thus causing significant inhibition of Ca^{2+} dependent inactivation of I_{Ca} . The principal reason for the different potencies of BAPTA and EGTA in reducing the rise of Ca^{2+} in the dyadic space was their different rates of Ca^{2+} binding (EGTA: $k_{on} = 5000 \text{ mM}^{-1} \text{ s}^{-1}$; BAPTA: $k_{on} = 500000 \text{ mM}^{-1} \text{ s}^{-1}$). As a consequence, the concentration gradients of free BAPTA and Ca^{2+} -BAPTA, and of free EGTA and Ca^{2+} -EGTA, between the dyadic space and bulk cytosol were substantially different (Fig 4) after the onset of depolarisation. In the case of BAPTA, large gradients provided large driving forces, causing rapid movement of Ca^{2+} -BAPTA molecules out of the dyadic space, and of free BAPTA into the dyadic space, so that BAPTA appeared to act as a fast ‘shuttle’. The slower rate of Ca^{2+} binding to EGTA, and the consequent development of substantially smaller free EGTA and Ca^{2+} -EGTA gradients between the dyadic space and cytosol, reduced the ability of EGTA to affect Ca^{2+} -induced inactivation of I_{Ca} .

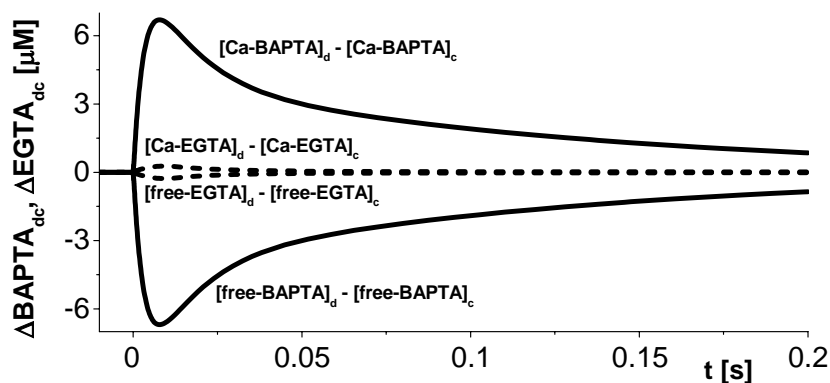


Fig 4. Gradients of BAPTA and EGTA with bound and unbound Ca^{2+} between dyadic (d) and cytosolic (c) space in the model.

5 Conclusion

The results of these simulations suggest that the different potencies of EGTA and BAPTA on inactivation of I_{Ca} are due to their different rates of Ca^{2+} binding, and thus different intracellular gradients of bound and unbound buffer, causing different rates of bound and unbound buffer diffusion out of and into the dyadic space. The consequent difference in suppression of the Ca^{2+} transient in the dyadic space caused different rates of Ca^{2+} - induced inactivation of I_{Ca} in the presence of the two buffers.

Acknowledgement

This work has been supported by the projects MSM0021622402 from the Ministry of Education, Youth and Sports of the Czech Republic, and AV0Z 20760514 from the Institute of Thermomechanics of Czech Academy of Sciences.

References

- [1] Brette F, Salle L, Orchard CH. Differential modulation of L-type Ca^{2+} current by SR Ca^{2+} release at the T-tubules and surface membrane of rat ventricular myocytes. *Circ Res* 2004; 95:e1-e7.
- [2] Sham JS. Ca^{2+} release-induced inactivation of Ca^{2+} current in rat ventricular myocytes: evidence for local Ca^{2+} signaling. *Journal of Physiology* 1997;500:285-295.
- [3] Pásek M, Šimurda J, Christé G. The functional role of cardiac T-tubules in a model of rat ventricular myocytes. *Phil Trans R Soc A* 2006;364:1187-1206.
- [4] Shannon TR, Wang F, Puglisi J, Weber C, Bers DM. A mathematical treatment of integrated Ca dynamics within the ventricular myocyte. *Biophys J* 2004;87:3351-3371.
- [5] Shannon TR, Bers DM. Assessment of intra-SR free [Ca] and buffering in rat Heart. *Biophys J* 1997;73:1524-1531.